Soft Matter

PAPER

Comparison of three competing dynamic force spectroscopy models to study binding forces of amyloid-β (1–42)†

Cite this: *Soft Matter*, 2014, **10**, 1924

F. T. Hane,[a] S. J. Attwood[b] and Z. Leonenko*[ab]

Received 23rd August 2013
Accepted 8th January 2014

DOI: 10.1039/c3sm52257a

www.rsc.org/softmatter

We performed single molecule dynamic force spectroscopy experiments to study the dimerization of two amyloid-β (1–42) peptides and compared three different theoretical models used to fit experimental data: Bell–Evans, Dudko–Hummer–Szabo, and Friddle–De Yoreo. Using these models we extracted values of the dissociation rate at zero force, k_0, and height and the width of the energy barrier, ΔG and x_β. We show the importance of including the effect of the linker molecule. All three models corrected for the linker effect give comparable results for x_β and show more discrepancy for k_0 and ΔG values, ΔG parameter correlates well between Dudko–Hummer–Szabo and Friddle–De Yoreo models but differs for the Bell–Evans model.

Introduction

Single molecule force spectroscopy (SMFS) is a nanoscale biophysical technique used to probe the unbinding of individual molecules or the unfolding of a polymer such as a protein[1,2] or nucleic acid.[3] By varying the loading rate, "dynamic force spectroscopy" (DFS) experiments can be conducted to extract thermodynamic and kinetic parameters.[2] A number of competing analytical models have been developed to extract the kinetic parameters such as the dissociation rate at zero force (also called the off rate), k_0,[4] and the thermodynamic parameters, x_β and ΔG, which are the width and height of the energy barrier, respectively.[4] These parameters are fundamental to the understanding of the kinetics and thermodynamics of the interaction of a pair of molecules and allow the comparison of kinetics between different systems and factors which may affect the affinity of two molecules. k_0 is a rate constant which is the inverse of the bond lifetime, τ_0, and measures the rate at which two molecules dissociate at zero force. The kinetic association rate (also referred to as the on rate), k_{on}, is the rate at which two molecules associate. By relating these two rates, the dissociation constant k_D, can be defined as $k_D = k_{off}/k_{on}$.[4] In this work, we present comparative analysis of the application of three different analytical models used to fit the same SMFS experimental data sets in an attempt to provide some standardization to the analysis of force spectroscopy experiments.

In a SFMS experiment, a molecule of interest is attached to a substrate *via* a heterobifunctional cross-linker molecule such as *N*-hydroxysuccinimide-polyethylene glycol-maleimide (NHS-PEG-MAL).[5] A complementary molecule is bound to the cantilever tip of the atomic force microscope (or to a bead in optical tweezers). The tip is brought in close proximity to the substrate allowing the two molecules to interact. The tip is retracted and the deflection of the AFM cantilever is measured as a function of the distance from the substrate. At rupture, the cantilever returns back to its original position and the rupture (or unbinding) force can be measured as a function of the cantilever deflection.

This technique has been used to probe the kinetics of unbinding for a diverse set of molecules from avidin–biotin interactions[2,4,6] to hydrocarbons.[7] A number of notable results have emerged from this technique: the force required to "unzip" the two complementary strands of DNA[8,9] and the reversible stretching and unfolding of a titin protein.[10]

Analytical models

To extract kinetic data from the unbinding experiments, a number of analytical models have been proposed to fit the experimental data. While the Bell–Evans model[11] is the oldest and most highly cited model, an argument can now be made questioning the interpretation of some experimental results which have utilized this model.[12]

Bell–Evans model

The Bell–Evans model was the result of Evans' adaptation of the work introduced by Bell in 1978[13] and adapted for atomic force spectroscopy (AFS).[11,14] This model posited that the rupture

[a]*Department of Biology, University of Waterloo, 200 University Ave West, Waterloo, ON, N2L 3G1, Canada*

[b]*Department of Physics and Astronomy, University of Waterloo, 200 University Ave West, Waterloo, ON, N2L 3G1, Canada. E-mail: zleonenk@uwaterloo.ca*

† Electronic supplementary information (ESI) available. See DOI: 10.1039/c3sm52257a

force between two cells was proportional to the natural logarithm of the loading rate during retraction. During a dynamic force spectroscopy (DFS) experiment, unbinding events are collected over a range of retraction velocities, and hence loading rates. These loading rates (the rate at which force is applied to the system) usually vary between 1000 and 100 000 pN s^{-1}. When the most probable unbinding force is determined from plotting all unbinding events at a given loading rate on a histogram, and the most probable unbinding force is plotted against the loading rate on a log scale, a straight line results, the slope of which is the location of the transition barrier and the *y*-intercept being the height of the energy barrier.[14] Using Bell–Evans equation (eqn (1)),[11,14]

$$F(r) = \left(\frac{k_B T}{x_\beta}\right) \ln \frac{r\, x_\beta}{k_0\, k_B T} \quad (1)$$

where $F(r)$ is the most probable rupture force, k_B, Boltzmann's constant, T, temperature in Kelvin, x_β, the location of the energy barrier, r, the loading rate, and k_0 the off rate constant at zero force. Once k_0 is determined, ΔG can be calculated using following equation (eqn (2)).[11]

$$-\Delta G = k_B T \ln \frac{k_0 h}{k_B T} \quad (2)$$

where h is Plank's constant.

Dudko–Hummer–Szabo model

Szabo and colleagues reduced the Bell–Evans model to its approximate limit using a stochastic model of a spring[15] and used Kramers' theory of diffusion[16] to determine kinetic constants. Szabo and colleagues later updated this model by adding an exponential constant of 1/2 to create a "cusp-like" model to better approximate kinetic parameters such as the kinetic off rate and location of the energy barrier.[17]

The Bell–Evans model assumes that $k_{off}(F)$ scales linearly with $\exp(Fx_\beta)$, so $k(F) = k_0 \exp(Fx_\beta)$. However, this assumption has been shown to be an oversimplification:[17] this phenomenological approximation holds as $\Delta G \rightarrow \infty$, but with ΔG of realistic values the unbinding process can be better modeled using Kramer's theory of diffusive barrier crossing. The Dudko–Hummer–Szabo model modifies the Bell–Evans model above and applied Kramer's theory to extract more rigorous kinetic and thermodynamic parameters.[15,17,18] In addition, Dudko showed that the molecular linker can be incorporated into the loading rate calculation.[18] The loading rate during a rupture event has been estimated as $r = k_c v$ where r is the loading rate (N s^{-1}), k_c the cantilever spring constant (N m^{-1}) and v the retract velocity (m s^{-1}).

Modifying the Bell–Evans model above, Szabo and colleagues determined an arbitrary exponential scaling constant to obtain the equation (eqn (3)),[17]

$$\tau(F) = \tau_0 \left(1 - \frac{aFx_\beta}{\Delta G}\right)^{1-1/a} e^{\frac{\Delta G}{}\left[1-\left(1-\frac{aFx_\beta}{\Delta G}\right)^{1/a}\right]} \quad (3)$$

where τ is the bond lifetime, a is a power scaling factor corresponding to 1/2 for a cusp-like barrier, 3/2 for a "linear-cubic barrier", and 1 for a recovery of the Bell–Evans model.

Dudko and colleagues showed that the loading rate of two molecules connected by a linker following worm like chain (WLC) dynamics can be modelled by eqn (4):

$$r(F) = v\left[\frac{1}{k_c} + \frac{2\beta L_c l_p (1 + \beta F l_p)}{3 + 5\beta F l_p + 8(\beta F l_p)^{5/2}}\right]^{-1} \quad (4)$$

where v is the retraction velocity, L_c is the contour length, β is $k_B T^{-1}$, and l_p is the persistence length of the system consisting of the linker and peptide. The persistence length is the length at which, when greater, the system deforms in a classical manner. The first term within the brackets represents the cantilever's contribution to the loading rate and the second term represents the molecular linker's contribution to the loading rate. The addition of the two terms is multiplied by the retraction velocity.

The bond lifetime, $\tau(F)$, is approximated by the eqn (5):

$$\tau(F) \cong \frac{\left[\frac{\pi}{2}\left(\langle F^2\rangle - \langle F\rangle^2\right)\right]^{1/2}}{r(F)} \quad (5)$$

where $\langle F^2\rangle$ is the mean squared rupture force at a given loading rate $r(F)$.

Often DFS experiments result in apparent multiple slopes in the unbinding force/loading rate plots.[19] Given early avidin–biotin experiments and their known multiple unbinding properties, experiments on simpler systems have also interpreted these non-linearity's as complex systems with multiple kinetic barriers with some barriers widths occurring at impossible distances of significantly less than 1 Å.[20]

Friddle–De Yoreo reversible binding model

Recently De Yoreo and colleagues challenged the assumption made by these earlier models that no reversible binding occurs during force experiments.[12] By challenging this assumption, De Yoreo was able to explain away some of the more peculiar conclusions reached by previous groups such as the complexity of very simple system and energy barriers of orders of magnitude less than 1 Å. As De Yoreo so aptly stated, "*If fitting is the only criterion, then the multi-barrier hypothesis can never be rejected, because this segmented approach can be tailored to fit any force spectrum*".

In the Friddle–De Yoreo interpretation, a system of two bodies being pulled apart passes through two phases: an equilibrium phase at lower pulling velocities where the molecules can rebind, and a kinetic phase at higher loading rates where molecules unbind irreversibly. The equilibrium phase is associated with a shallow slope and the kinetic phase, a steeper slope.

The force at which the dissociation rate and the association rate cross is given by the equilibrium equation,

$$f_{eq} = \sqrt{2k_c \Delta G} \quad (6)$$

where k_c is the spring constant of the cantilever and ΔG the height of the activation barrier.

The unbinding force, $F(r)$, is approximated by the equation,

$$F(r) \cong f_{eq} + f_\beta \ln\left(1 + \frac{re^{-\gamma}}{k_{off}(f_{eq})f_\beta}\right) \quad (7)$$

where γ is Euler's constant, 0.577. The thermal force scale, f_β is given by the expression $f_\beta = k_B T/x_\beta$. $k_{off}(f_{eq})$ is the dissociation rate at the equilibrium force, f_{eq}, the force at which the system transitions from the equilibrium regime to the kinetic regime. $F(r)$ is the mean rupture force as a function of the loading rate, r, corrected for the effect of the PEG linkers as demonstrated in ref. 18.

From f_β, the width of the energy barrier, x_β, can be calculated as,

$$x_\beta = \frac{k_B T}{f_\beta} \quad (8)$$

The dissociation rate at force F, k_{off} (F) is given by the function,

$$k_{off}(F) = k_0 \exp[\beta(Fx_\beta - 1/2k_c{x_\beta}^2)] \quad (9)$$

The association rate (on-rate), $k_{on}(F)$, is given by the function,

$$k_{on}(F) = k_{on}(0)\exp\left[-\frac{\beta k_c}{2}\left(\frac{F}{k_c} - x_\beta\right)^2\right]$$

$$k_{on}(F) = k_0 \exp\left[\beta\left(\Delta G - \frac{F^2}{2k_c}\right)\right] \quad (10)$$

Amyloid-β binding

Amyloid-β is a 35–42 amino acid long peptide which is associated with the symptoms associated with Alzheimer's disease. During the Alzheimer's pathological process, amyloid-β monomers aggregate to form dimers leading to neurotoxic higher order oligomeric structures including annular protofibrils (APF's)[21] and prefibrillar oligomers (PFO's).[22] Amyloid oligomers have been shown to be more neurotoxic than the insoluble fibrils.[23,24] It is believed that these aggregates form ion pores leading cellular dyshomeostasis[25] or thin the membrane leading to distorted bilayer conductance.[26] In addition, a number of other methods of amyloid toxicity have been demonstrated including the oxidative stress to the cell membrane mediated by metal ions[27] and lipid peroxidation caused by reactive oxidative species.[28]

In this work we use atomic force spectroscopy to extract unbinding force data for amyloid-β (1–42). We then apply the three models described (Bell–Evans, Dudko–Hummer–Szabo, Friddle–De Yoreo) in a variety of iterations to our AFS data to extract kinetic and thermodynamic data about the rupture of the amyloid-β dimer, the smallest toxic form of the amyloid oligomer.[29,30]

Results and discussion

Force curves were collected at a variety of retraction velocities and plotted as histograms with respect to the average loading rate, $r(F) = vk_c$ here k_c is the cantilever spring constant and v the retraction velocity (Fig. 1). The most probable rupture force as a function of loading rate is consistent with our previous reports.[5,31] We noted that the distribution of our unbinding forces contained within our histograms broaden with increasing loading rate which is consistent with theoretical and experimental models.[18]

Bell–Evans model

In Fig. 2A we plotted the most probable rupture forces against the uncorrected loading rate retraction velocity (nm s^{-1}) times cantilever spring constant (nN m^{-1}) (Fig. 2A). A least-squares linear fit was calculated to best approximate a straight line through the data points (Fig. 2A). This line through the data when placed on a natural logarithm scale is consistent with what is predicted by Evans.[11,14] Parameters of the line were calculated by the graphing software and calculated as a slope of 2.84×10^{-11} and an intercept of 5.34×10^{-10}. We applied the Bell–Evans model to these line parameters to calculate the following parameters: $x_\beta = 143$ pm, $k_0 = 240.3$ s^{-1}, and $\Delta G = 24.0$ $k_B T$ (Fig. 2A).

Dudko–Hummer–Szabo model

Using the eqn (5), we calculated the bond lifetime, $\tau(F)$ for each bin with mean force, F. We calculated the natural logarithm of $\tau(F)$ and plotted this against the rupture force, F, as shown in Fig. 2B. We applied the Dudko–Hummer–Szabo model (eqn (3)) and fit this equation to our data.[18] Applying the Dudko–Hummer–Szabo cusp model to our data of the rupture of two Aβ42 peptides, we extracted the fitting parameters of $x_\beta = 205$ pm, $k_0 = 0.68$ s^{-1}, and $\Delta G = 7.7$ $k_B T$.

Friddle–De Yoreo model

To obtain kinetic parameters using the Friddle–De Yoreo model,[12] we plotted the mean unbinding force $F(r)$as a function of the loading rate for each set of loading rates as shown in Fig. 2C and D. The Friddle–De Yoreo reversible binding equation was fit to the data and fitting parameters k_{off}, f_{eq} and f_β were calculated (Fig. 2C and D). The equilibrium force, f_{eq}, was calculated to be 38.4 pN. Thermodynamic parameters x_β and ΔG were obtained by rearranging eqn (6)–(8). Using the Friddle–De Yoreo model, we obtained values of $k_0 = 11.1$ s^{-1}, $x_\beta = 104$ pm and $\Delta G = 7.5$ $k_B T$.

A summary of kinetic parameters extracted using different models is given in Table 1.

Discussion

Comparing the results of these different models and their various iterations, a few important observations stand out. Firstly, a large variation in the dissociation rates between those models which do not correct for the effect of the PEG linker and those that do shows that correcting the loading rate for the effect of the PEG linker is very important for determining accurate dissociation rates although it is minimally important for determining thermodynamic parameters. Secondly, the Friddle–De Yoreo and Dudko–Hummer–Szabo model show

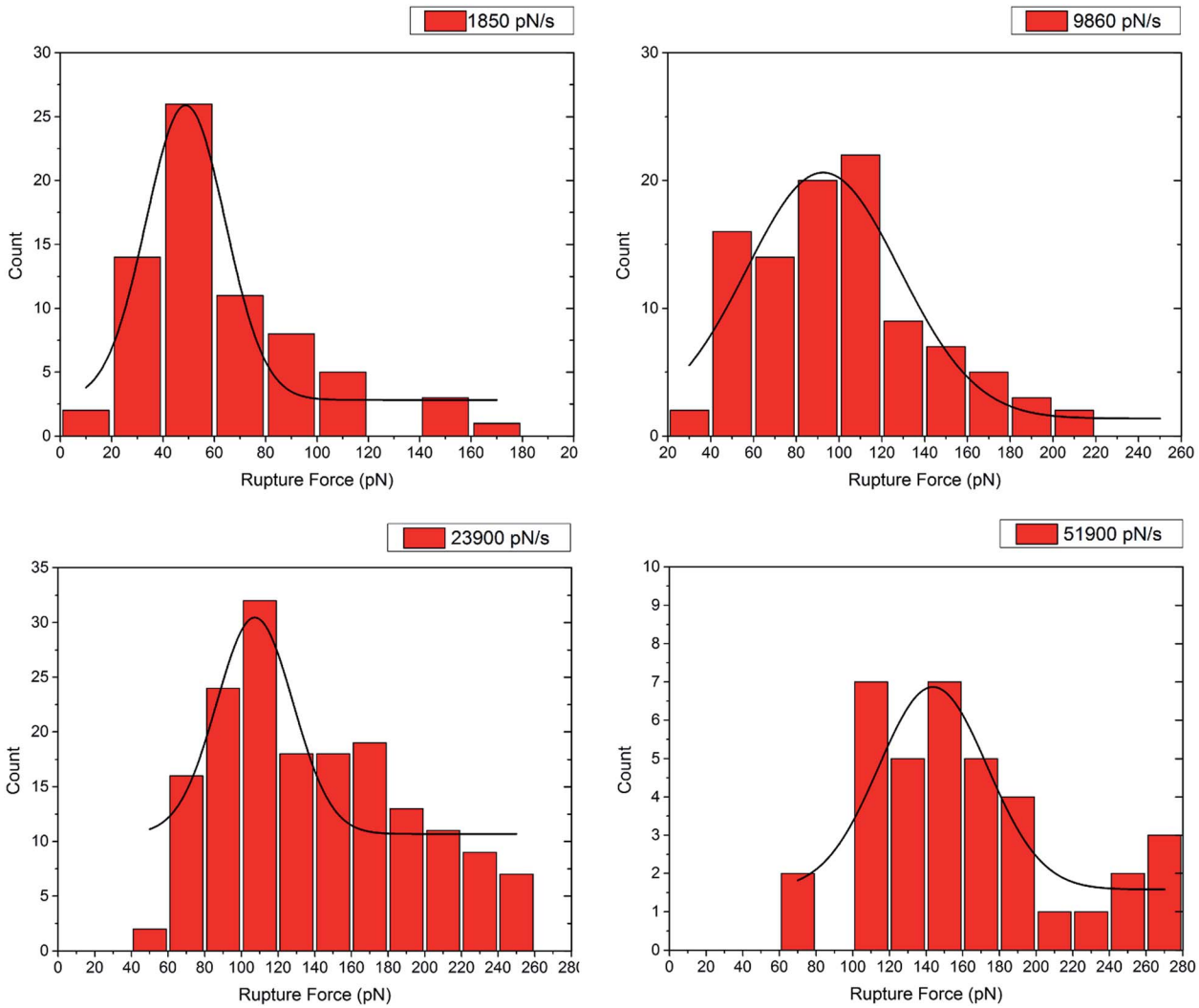

Fig. 1 Rupture force histograms and Gaussian fit at corrected loading rates of 1950 pN s^{-1}, 9860 pN s^{-1}, 23 900 pN s^{-1} and 51 900 pN s^{-1}.

similar energy barrier heights, ΔG. Lastly, the width of the energy barrier, x_β, is similar for all models.

It appears that no two models provide near sufficiently similar results to definitively rule out the third model. So which model provides the most rigorous results? Clearly any model that does not account for the effect of the linker molecule is bound to calculate dissociation rates which are erroneous by several orders of magnitude. The Friddle–De Yoreo model relies on fewer assumptions than the other two models, namely that reversible binding of the two peptides. Together with our data that demonstrate an exponential line of best fit rather than two linear fits, we conclude that the Friddle–De Yoreo model provides a superior analysis of the kinetics of unbinding of two molecules than the Bell–Evans model.

Given the variance between SMFS experiments conducted under identical conditions, we suggest that the scientific value of SMFS is not to obtain absolute kinetic and thermodynamic parameters of a given system, but rather serves as a tool to compare two or more different experiments or how a variable affects these parameters.

Early force spectroscopy experiments were conducted on the avidin–biotin system, a system known to have complex (ie more than one) binding conformation.[19,32] When force spectra were collected for this system, multiple lines of best fit were found which were plausibly interpreted as multiple energy barriers with each barrier corresponding to a different method of unbinding. However this interpretation remained popular even though some systems are much simpler than the avidin–biotin complex such as peptides on steel.[33] It is highly unlikely that these systems contain the complex kinetics of the avidin–biotin receptor–ligand pair. Much of this force spectroscopy data have been interpreted as a complex energy landscape containing multiple barriers even when the system involves very simple binding such as peptide to steel[33] or when the energy barrier is shown to be sub-angstrom by multiple orders of magnitude.[20] Friddle and colleagues provided an alternate interpretation to account for the exponential shape of the rupture force plot which does not require multiple fits to straight lines as the Bell–Evans model does.

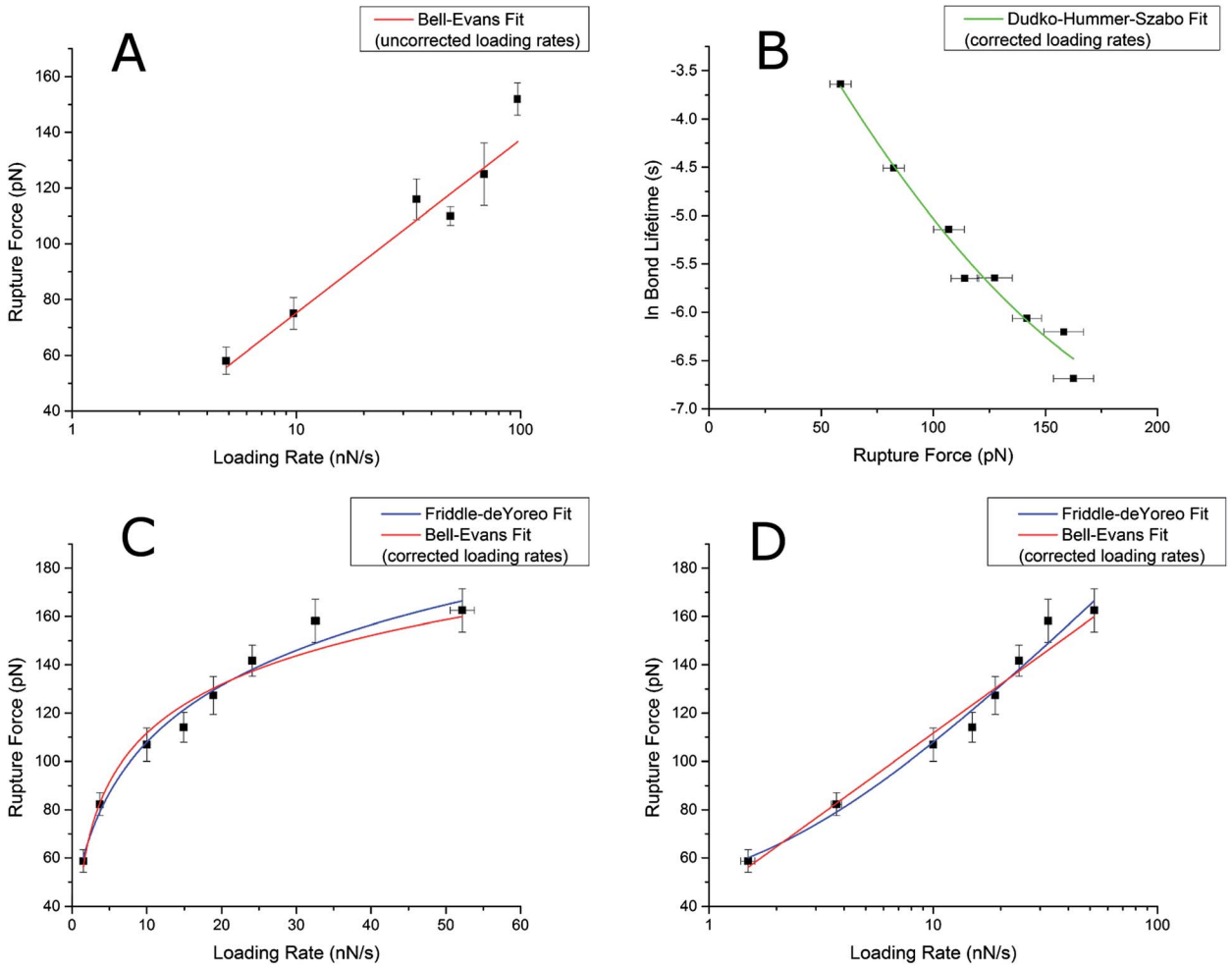

Fig. 2 (A) Rupture force *vs.* loading rate using the Bell–Evans model. Most probable rupture forces are plotted against the uncorrected loading rate. Each data point corresponds to the most probable rupture force for an experiment conducted at a given retraction velocity. Retraction velocity is converted to loading rate by multiplying by the cantilever spring constant. A straight line Bell–Evans model is fit to the data and the *y*-intercept and slope is calculated. The adjusted R^2 value was calculated as $R^2 = 0.973$. (B) Bond lifetime *vs.* rupture force fit with the Dudko–Hummer–Szabo model (green) applied to all force curves binned into 8 bins in accordance with corrected loading rate. $\chi^2 = 0.031$. (C and D) Aβ unbinding experimental data fitted with the Friddle–De Yoreo reversible binding model (blue) and the Bell–Evans model (red). Data and analysis are identical, but (C) is on base 10 scale and (D) is on a log10 scale. All data points are binned linker-corrected loading rates. The data used in this graph are identical to that shown in Fig. 2A, however all force curves were sorted in order of corrected loading rate and binned into 1 of 8 bins according to the corrected loading rate. $R^2 = 0.973$ for the Bell–Evans (red) model and $R^2 = 0.979$ for the Friddle–De Yoreo (blue) model.

While we do not claim that the Bell–Evans model lacks accuracy or rigour for a simple system, we share the concerns noted by Friddle and believe that many reports have "over-interpreted" the Bell–Evans model and calculated multiple energy barriers where none can plausibly exist, such as at sub-Angstrom length scales.

Table 1 Comparison of kinetic and thermodynamic parameters using different force spectroscopy models. Different iterations of each model are described in methods section

DFS Model	x_β (pm)	ΔG (k_BT)	k_0 (s^{-1})	τ_0 (s)
Bell–Evans (uncorrected for PEG linkers)	143 ± 16.9	24.0 ± 3.6	240.3 ± 36.5	0.00416 ± 0.0006
Bell–Evans (loading rates corrected for PEG linker)	143 ± 16.4	27.3 ± 4.1	8.44 ± 1.2	0.112 ± 0.02
Bell–Evans (binned - loading rates corrected)	138 ± 9.7	27.5 ± 2.5	7.14 ± 0.6	0.14 ± 0.01
Bell–Evans (aggregate data)	136 ± 9.4	27.4 ± 2.5	7.55 ± 0.7	0.132 ± 0.01
Dudko–Hummer–Szabo (cusp model)	205 ± 51.7	7.7 ± 0.2	0.68 ± 0.4	1.47 ± 0.9
Friddle–De Yoreo (binned data)	104.2 ± 19.3	7.50 ± 2.7	11.1 ± 7.4	0.090 ± 0.06
Friddle–De Yoreo (aggregate data)	98.9 ± 19.6	7.83 ± 3.0	12.5 ± 8.5	0.080 ± 0.05

In summary, we report that three models we used (corrected for the linker effect) give comparable results for x_β and k_0, while ΔG parameter correlates well between Dudko–Hummer–Szabo and Friddle–De Yoreo models but differs for the Bell–Evans model. Despite some variation in results due to applying different models, SMFS experiments are very useful to measure the binding forces, as well as to extract kinetic and thermodynamic parameters of the system. These studies are especially useful to evaluate the effect of various factors on binding events. Although a careful consideration of the analytical model applied to fit experimental data should be made to make a correct comparison. We share the opinion of De Yoreo in that multiple slopes in the force-loading rate plots are likely the result of rebinding events and not a multiple energy barrier, especially in simple systems, such as the one we have studied.

Experimental procedures

We used the protocol as described previously.[5,31] Briefly, Veeco MLCT Silicon Nitride AFM cantilevers were cleaned using ethanol and UV light. The tips and freshly cleaved mica were soaked in aminopropylsilatrane (APS) to silanate the surface to prepare for PEG linker attachment followed by soaking in a solution of 3400 MW NHS-PEG-MAL (Laysan Bio, Alabaster GA) solution. A solution of 20 nM cys-amyloid-β (1-42) was prepared in HEPES 50 mM buffer (pH 7.4, 150 mM NaCl) and soaked on the surface of the cantilever tip and mica surface. Following rinsing, unreacted maleimide groups were quenched with β-merceptoethanol. Tips and mica were then rinsed and stored in HEPES buffer.

Atomic force spectroscopy

We used a JPK Nanowizard II atomic force microscope for all measurements. Cantilever spring constants were measured using Hutter's thermal tune method.[34] Typical spring constant values of cantilevers were between 24 and 170 mN m^{-1} but varied with each experiment. Mica coated with amyloid-β was placed on the stage in the liquid cell and immersed in HEPES buffer. A series of force curves were taken with an approach and retract velocities of 200, 400, 2000, and 4000 nm s^{-1} resulting in loading rates between 4500 pN s^{-1} and 98 000 pN s^{-1}. A dwell time of 0.5 seconds was set to allow peptide–peptide binding events. All experiments were conducted at room temperature (293 K). For a single experiment approximately 1000 force curves were recorded, out of which approximately 5–10% of these showed specific unbinding events. 5 data sets were collected each using a different cantilever chip. 3 data sets were collected with the same cantilever and 2 others were collected with a softer cantilever.

Force curve analysis

JPK data analysis software was used to analyze force curves. Software functions were used to smooth the force curves, level the x-axis, set both axis to 0 and obtaining the tip sample separation, z, to correct for cantilever deflection. A worm-like-chain (WLC) fit was obtained for each force curve and rupture forces were obtained. Data was truncated using Poisson statistics to eliminate force curves that were likely the result of simultaneous multiple unbind events as described in.[35] These rupture forces were plotted as histograms at the different collected loading rates and fitted with a Gaussian distribution to determine the most probable rupture force. Errors quoted for the most probable rupture force are evaluated as the standard deviation of each distribution, divided by the square root of the effective number of counts for each distribution (estimate of standard error).

Kinetic and thermodynamic parameters k_0, ΔG and x_β were extracted using a number of different dynamic force spectroscopy models.

Extraction of kinetic data

Bell–Evans model. Kinetic parameters for the uncorrected Bell–Evans model were calculated by plotting the most probable rupture force (obtained from histograms) against the natural logarithm of the loading rate calculated by multiplying the cantilever spring constant k_c, by the retraction velocity, v. A straight line was fit to the data using a least squares regression model using Origin v. 9.0 software. The software returned values of R^2 and χ^2 for linear and non-linear fits, respectively, to indicate the quality of the fit to the experimental data. The calculated slope and the y-intercept of this line were used to extract k_0, ΔG and x_β using the Bell–Evans eqn (1) and (2). In another iteration of the application of this model, we corrected the loading rate for the effect of the PEG linkers by applying eqn (4) as described in[18] to calculate the corrected loading rate and reapplied the above described procedure to obtain k_0, ΔG and x_β. In the third iteration, we aggregated the results of all our force curves and equally divided the data into 8 bins according to their corrected loading rates. The most probable rupture force and mean corrected loading rate were calculated for each bin and plotted (Fig. 2C and D). Once again, we applied the Bell–Evans model to determine k_0, ΔG and x_β. In the last iteration of the application of this model (referred to as aggregate data), the results of all force curves were plotted (about 500 force data points) and the Bell–Evans model applied to the all force plot data points.

Dudko–Hummer–Szabo model. All force curves were collected and binned into 8 bins according to their corrected loading rate as described above. We plotted the natural logarithm of the corrected loading rate of each bin *vs.* the rupture force of each bin, to obtain the bond lifetime *versus* rupture force relationship as show in Fig. 2B. The Dudko–Hummer–Szabo model was fit to the data using a Levenberg–Marquardt fitting algorithm using the software's user defined non-linear fitting function. The bond lifetime, τ_0, ΔG and x_β, were returned by the software. k_0 was determined by the inverse relationship $k_0 = 1/\tau_0$.

Friddle–De Yoreo model. Rupture force, $F(r)$ *versus* corrected loading rate, r, data points were binned and plotted as described above (Fig. 2C and D). We fit the Friddle–De Yoreo reversible binding equation to these data points and extracted parameters equilibrium force, f_{eq}, thermal scaling factor, f_β, and

dissociation rate, $k_{off}(f_{eq})$ at the equilibrium force. These parameters were then used to calculate parameters ΔG, x_β, and k_0 using the equations used in (Friddle, 2011). In the last iteration of the application of this model, we plotted all force curve data points (approximately 500 data points) and fit the Friddle–De Yoreo model to the entirety of our data to obtain the parameters from the fitting of the Friddle–De Yoreo equation to this data set.

Conclusions

Our data demonstrated that correcting the loading rate for the effect of the linker molecule is imperative for accurately determining dissociation rates. All three models corrected for the linker effect give comparable results for x_β and show more discrepancy for k_0 and ΔG values. ΔG parameter correlates better between Dudko–Hummer–Szabo and Friddle–De Yoreo models but differs for the Bell–Evans model. Due to these discrepancies more independent experiments by other methods or simulations are needed in order to confirm which model is better. Based on our data we conclude that Friddle–De Yoreo model provides a better fit for experimental data and is more suitable for the analysis of kinetics of unbinding events. Despite some variation in absolute numbers for x_β, k_0 and ΔG, due to applying different models, DFS experiments are very useful, especially to evaluate the effect of various factors on binding events.

Acknowledgements

The authors wish to thank Prof. Scott Taylor (University of Waterloo) for synthesis of APS, Melesa Hane for critical reading of the manuscript and Prof. Arvi Rauk (University of Calgary) for helpful discussions. Funding from Natural Sciences and Engineering Research Council of Canada (NSERC), Canadian Foundation for Innovation (CFI), Ontario Research Fund (ORF) and University of Waterloo is greatly acknowledged.

Notes and references

1 E. Florin, V. Moy and H. Gaub, *Science*, 1994, **264**, 415.
2 P. Hinterdorfer and F. Dufrêne, *Nat. Methods*, 2006, **3**, 347.
3 J. Liphardt, S. Dumont, S. Smith, I. Tinoco and C. Bustamante, *Science*, 2002, **296**, 1832.
4 A. Bizzarri and S. Cannistraro, *Chem. Soc. Rev.*, 2010, **39**, 734.
5 F. Hane, G. Tran, S. Attwood and Z. Leonenko, *PLoS One*, 2013, **8**, e59005.
6 P. Hinterdorfer, W. Baumgartner, H. Gruber, K. Schilcher and H. Schindler, *Proc. Natl. Acad. Sci. U. S. A.*, 1996, **93**, 3477.
7 C. Ray, J. Brown and B. Akhremitchev, *J. Phys. Chem. B*, 2006, **110**, 17578.
8 G. Lee, L. Chrisey and R. Colton, *Science*, 1994, **266**, 771.
9 T. Boland and B. D. Ratner, *Proc. Natl. Acad. Sci. U. S. A.*, 1995, **92**, 5297.
10 M. Rief, M. Gautel, F. Oesterhelt, J. Fernandez and H. Gaub, *Science*, 1997, **276**, 1109.
11 E. Evans and K. Ritchie, *Biophys. J.*, 1997, **72**, 1541.
12 R. Friddle, A. Noy and J. De Yoreo, *Proc. Natl. Acad. Sci. U. S. A.*, 2012, **109**, 13573.
13 G. Bell, *Science*, 1978, **200**, 618.
14 E. Evans, *Annu. Rev. Biophys. Biomol. Struct.*, 2001, **30**, 105.
15 G. Hummer and A. Szabo, *Biophys. J.*, 2003, **85**, 5.
16 H. Kramers, *Physica*, 1940, **7**, 284.
17 O. Dudko, G. Hummer and A. Szabo, *Phys. Rev. Lett.*, 2006, **96**, 108101.
18 O. Dudko, G. Hummer and A. Szabo, *Proc. Natl. Acad. Sci. U. S. A.*, 2008, **105**, 15755.
19 R. Merkel, P. Nassoy, A. Leung, K. Richie and E. Evans, *Nature*, 1999, **397**, 50.
20 A. Berquand, N. Xia, D. Castner, B. Clare, N. Abbott, V. Dupres, Y. Adriaensen and Y. Dufrêne, *Langmuir*, 2005, **21**, 5517.
21 R. Kayed, A. Pensalfini, L. Margol, Y. Sokolov, F. Sarsoza, E. Head, J. Hall and C. Glabe, *J. Biol. Chem.*, 2009, **284**, 4230.
22 C. Glabe, *J. Biol. Chem.*, 2008, **283**, 29639.
23 R. Kayed, E. Head, J. Thompson, T. McIntire, S. Milton, C. Cotman and C. Glabe, *Science*, 2003, **300**, 486.
24 A. Quist, I. Doudevski, H. Lin, R. Azimova, D. Ng, B. Frangione, B. Kagan, J. Ghiso and R. Lal, *Proc. Natl. Acad. Sci. U. S. A.*, 2005, **102**, 10427.
25 H. Lin, R. Bhatia and R. Lal, *FASEB J.*, 2001, **15**, 2433.
26 Y. Sokolov, A. Kozak, R. Kayed, A. Chanturiya, C. Glabe and J. Hall, *J. Gen. Physiol.*, 2006, **128**, 637.
27 L. Sayre, G. Perry and M. Smith, *Curr. Opin. Chem. Biol.*, 1999, **3**, 220.
28 E. Mutisya, A. Bowling and M. Beal, *J. Neurochem.*, 1994, **63**, 2179.
29 K. Ono, M. Condron and D. Teplow, *Proc. Natl. Acad. Sci. U. S. A.*, 2009, **106**, 14745.
30 B. Barz and B. Urbanc, *PLoS One*, 2012, **7**, e34345.
31 B. Kim, N. Palermo, S. Lovas, T. Zaikova, J. Keana and Y. Lyubchenko, *Biochem. J.*, 2011, **50**, 5154.
32 O. Livnah, E. Bayer, M. Wilchek and S. Sussman, *Proc. Natl. Acad. Sci. U. S. A.*, 1993, **90**, 5076.
33 J. Landoulsi and V. Dupres, *ChemPhysChem*, 2011, **12**, 1310.
34 J. Hutter and J. Bechhoefer, *Rev. Sci. Instrum.*, 1993, **64**, 1868.
35 O. Karácsony and B. Akhremitchev, *Langmuir*, 2011, **27**, 11287.

Soft Matter

ARTICLE

Electronic Supplementary Information

Bell-Evans Calculations

The Bell-Evans equation[1] is expanded to obtain a similar form to the straight line equation y=mx+c,

$$F(r) = \left(\frac{k_B T}{x_\beta}\right) \ln r + \left(\frac{k_B T}{x_\beta}\right) \ln \frac{x_\beta}{k_{off}\, k_B T}$$

Therefore when F(r) is plotted against ln r, the slope of the best fit line equals $\left(\frac{k_B T}{x_\beta}\right)$ and the y-intercept equals $\left(\frac{k_B T}{x_\beta}\right) \ln \frac{x_\beta}{k_{off}\, k_B T}$.

All values are converted to standard units, N and N/s. The width of the energy barrier, x_β is determined by the equation,

$$x_\beta = \frac{k_B T}{m}$$

Where m is the slope of the line. k_{off} was determined by rearranging the equation.

$$k_{off} = \frac{x_\beta}{k_B T\, e^{c x_\beta / k_B T}}$$

Where c is the y-intercept.

Once k_{off} is determined, we applied the following equation to determine the height of the energy barrier, ΔG[1].

$$k_{off}\,(F) = \left(\frac{k_B T}{h}\right) e^{-\frac{\Delta G - x_\beta F}{k_B T}}$$

Rearranged, ΔG can be determined as

$$-\Delta G = k_B T \ln \frac{k_0 h}{k_B T}$$

Where h is Plank's constant. For our purposes, we used $k_B T$ as units for ΔG.

Error Analysis

For the Bell-Evans model, errors were determined by the square root of the sum of the squares of the standard error[2]. For example, the standard error of x_β was calculated as follows:

Since x_β is a function of the slope, m,

$$x_\beta = \frac{k_B T}{m}$$

With m being the slope of the line using a least squares fit of the data points, the standard error of x_β is given by the equation,

$$\frac{\delta x_\beta}{x_\beta} = \sqrt{\left(\frac{\delta m}{m}\right)^2 + \left(\frac{\delta T}{T}\right)^2}$$

The standard error of the slope, m, was calculated using the graphing software. The standard error of the temperature was negligible, but still used and estimated as 1 K.

The standard error for all parameters using the Dudko-Hummer-Szabo model[3] were calculated using Origin v 9.0.

Hutter's thermal noise method[4] of cantilever spring constant calculation typically results in a standard error of 10-20%[5]. To calculate the standard errors for the Friddle-De Yoreo model[6], a 15% error was estimated for the cantilever spring constant. Since ΔG is a function of the cantilever spring constant and f_{eq}, the standard error in ΔG was estimated as

$$\delta \Delta G = \Delta G \sqrt{\left(\frac{\delta f_{eq}}{f_{eq}}\right)^2 + 0.15^2}$$

The remainder of standard errors were calculated in a manner similar to the Bell-Evans model.

Supplementary Information References

1 E. Evans, and K. Ritchie, *Biophys J.* 1997, **72**, 1541.

2 J. Taylor J. An Introduction to Error Analysis, 1997, Sausalito: University Science Books.

3 O. Dudko, G. Hummer, and A. Szabo A, *Proc. Nat. Acad. Sci.,* 2008, **105**, 15755.

4 J. Hutter, and J. Bechhoefer, *Rev. Sci. Instrum*., 1993, **64**, 1868.

5 JPK Instruments AG. Technical Summary: Calibration of atomic-force microscope tips.

6 R. Friddle, A. Noy, and J. De Yoreo, *Proc. Nat. Acad. Sci. USA*., 2012, **109**, 13573.